

# EFFECT OF THE DENSITY OF INUNDATION WATER ON TSUNAMI RUN-UP

Hideo Matsutomi<sup>1</sup>

Aiming for the advancement of historical and/or prospective tsunami scale evaluations, and focusing on the tsunami run-up, series solutions to the tip position  $a(t)$ , velocity  $U (=da/dt)$  and acceleration  $d^2a/dt^2$  in the tip region of inundation flow (unsteady flow) with sediment over a uniformly sloping bottom under the condition that the friction factor  $K$  is not linked to the density  $\rho$  of inundation water, and analytical solutions to  $a(t)$ ,  $U(t)$ ,  $d^2a/dt^2$ , the maximum run-up distance  $a_m$  and height  $R_m$  under the condition that  $K$  is linked to  $\rho$  are derived, and effects of  $\rho$  on them and run-up process are theoretically examined. It is indicated that (1) in the run-up analysis (including numerical simulation) of tsunami with sediment under the condition of a constant  $K$ , even if  $a_m$  and  $R_m$  can be predicted accurately, there is a possibility of evaluating the run-up duration time inaccurately and *vice versa*, and (2) linking  $K$  to  $\rho$  is necessary to solve this matter. An expression for the relationship between  $K$  and  $\rho$  is also presented. Moreover, it is verified that the derived series and analytical solutions are useful to discuss the effects of  $\rho$  on the run-up of tsunami with sediment through a comparison between the experimental and theoretical maximum run-up distances.

*Keywords: density of inundation water; tsunami; series and analytical solutions*

## INTRODUCTION

Aiming for the advancement of the tsunami load, and historical and/or prospective tsunami scale evaluations, the dependency of the density  $\rho$  of inundation water on hydraulic quantities such as incident Froude number  $F_{ris}$  and the dependencies of the maximum tsunami run-up distance, sediment deposit distance, etc. on  $\rho$  were examined through a small-scale hydraulic experiment (Matsutomi and Konno 2019). However, scale effects are feared, as is usual with a small-scale experiment. A solution to this matter is to examine target problems theoretically.

In this study, focusing on the tsunami run-up, solutions to the tip position  $a(t)$ , velocity  $U(t)$ , run-up height  $R_m$  and so on of inundation flow (unsteady flow) with sediment over a uniformly sloping bottom are derived theoretically, effects of  $\rho$  on them and run-up process of inundation flow are examined, and knowledge concerning them is enhanced as a result.

## THEORY

Initial condition (incident bore condition at a shoreline) of objective tsunami inundation flow and the definition of main symbols are shown in Figure 1. The incident inundation flow is Shen *et al.*'s (1963) and Peregrine *et al.*'s (2001) dam break flow which can express tsunami or wave run-up and backwash processes and has been utilized for, e.g., evaluations of the volume of wave overtopping (Peregrine *et al.* 2001) and sediment movement in the swash zone (Kelly *et al.* 2010). Hydraulic resistance is introduced after Whitham (1955) to take sediment in the tip region ( $=a(t)-\xi(t)$ . See Figure 1), and inundation flow velocity  $U (=da/dt)$  in the tip region is assumed to be a function of time alone.

The conservation law of mass  $M$  in the tip region of inundation flow with the bottom friction (or sediment) could be expressed as follows (refer to Matsutomi 1985):

$$\frac{dM}{dt} = \int_{\xi}^{x_s} \frac{d(\rho h_p)}{dt} dx - (\rho h_p)_{x=\xi} \frac{d\xi}{dt} = \frac{d}{dt} \int_{\xi}^{x_s} \rho h_p dx \quad (1)$$

where  $t$  is the time,  $x$  the distance axis along the slope,  $x_s(t)$  and  $h_p(t)$  the tip position and local water depth of inundation flow without sediment respectively,  $\xi(t)$  and  $\rho$  the rear position and the density of inundation water of the tip region of inundation flow with sediment respectively. Although inflow mass from the rear position  $\xi(t)$  into the tip region is that of water without sediment, it is assumed in this model that density of the inflow water becomes the same as the density  $\rho$  of inundation water in the tip region immediately after the inflow by taking sediment from the bottom (a movable bed) and the same volume of water without sediment as volume of sediment taken from the bottom is left on the bottom.

When  $K$  is a friction factor of inundation flow on a movable bed (Matsutomi 2019), the conservation law of momentum  $P$  in the tip region of inundation flow could be expressed as follows:

$$\frac{dP}{dt} = U \frac{d}{dt} \int_{\xi}^{x_s} \rho h_p dx + \frac{1}{2} \rho_w g H^2 - igM - \rho K U^2 (a - \xi) \quad (2)$$

where  $\rho_w$  is the density of water without sediment,  $g$  the gravitational acceleration,  $H(t)$  the inundation water depth at  $\xi(t)$ ,  $i$  the bottom slope and  $a(t)$  the tip position of inundation flow with sediment. In

<sup>1</sup> Research and Development Initiative, Chuo University, 1-13-27 Kasuga, Bunkyo-ku, Tokyo, 112-8551, Japan

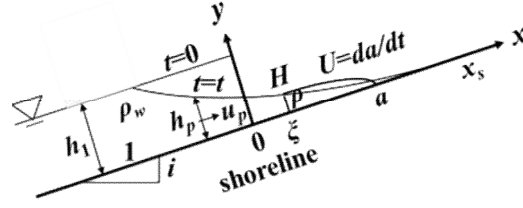


Figure 1. Initial condition and definition of main symbols.

Equation (2), the right side first term includes inflow of momentum originated from the bottom sediment. As the right side second term is a total hydrostatic pressure of inundation water without sediment, a discontinuity of total hydrostatic pressure at  $\zeta(t)$  may be imagined. In this study, it is assumed that as the density  $\rho$  of inundation water in the tip region is a space averaged, the total hydrostatic pressure at  $\zeta(t)$  is continuous.

Using the relation  $P=MU$  derived from the stated assumption that inundation flow velocity  $U(t)$  in the tip region is a function of time alone, Equations (1) and (2) become

$$\left[ \int_{\xi}^{x_s} h_p dx \right] \frac{dU}{dt} = \frac{1}{2} \frac{\rho_w}{\rho} g H^2 - ig \left[ \int_{\xi}^{x_s} h_p dx \right] - KU^2(a - \xi) \quad (3)$$

Inundation water depth  $h_p$  and inundation flow velocity  $u_p$  of Shen *et al.*'s and Peregrine *et al.*'s dam break flow at an arbitrary time  $t$  and position  $x$  are expressed as follows:

$$h_p = \frac{1}{9g} \left( 2c_1 - \frac{x}{t} - \frac{1}{2}igt \right)^2 \quad (4) \quad u_p = \frac{2}{3} \left( c_1 + \frac{x}{t} - igt \right) \quad (5)$$

where  $c_1 = \sqrt{gh_1}$  and  $h_1$  an initial constant stored water depth at a dam (an incident bore height at a shoreline). Therefore, the inundation water depth  $H(t)$  and inundation flow velocity  $U(t)$  at the rear position  $\zeta(t)$  of the tip region of inundation flow become

$$H = \frac{1}{9g} \left( 2c_1 - \frac{\xi}{t} - \frac{1}{2}igt \right)^2 \quad (6) \quad U = \frac{2}{3} \left( c_1 + \frac{\xi}{t} - igt \right) \quad (7)$$

From Equations (4) and (7), the tip position  $x_s$  of inundation flow without sediment and the rear position  $\zeta(t)$  of inundation flow with sediment are expressed as follows:

$$x_s = 2c_1 t - \frac{1}{2}igt^2 \quad (8) \quad \xi = \left( \frac{3}{2}U - c_1 + igt \right) t \quad (9)$$

Therefore, the basic equation for the tip position  $a(t)$  of inundation flow with sediment becomes

$$\left( c_1 - \frac{1}{2} \frac{da}{dt} - \frac{1}{2}igt \right)^3 t \frac{d^2a}{dt^2} - \frac{1}{2} \frac{\rho_w}{\rho} \left( c_1 - \frac{1}{2} \frac{da}{dt} - \frac{1}{2}igt \right)^4 + ig \left( c_1 - \frac{1}{2} \frac{da}{dt} - \frac{1}{2}igt \right)^3 t + Kg \left\{ a - \left( \frac{3}{2} \frac{da}{dt} - c_1 + igt \right) t \right\} \left( \frac{da}{dt} \right)^2 = 0 \quad (10)$$

Equation (10) is final basic equation to be solved in this study and is solved under two different conditions that the friction factor  $K$  is not linked (series solution) and is linked (analytical solution) to the density  $\rho$  of inundation water, without introducing a threshold of sediment movement.

When inundation flow has no sediment,  $\rho/\rho_w=1$  and Equation (8) is derived from Equation (10).

### SERIES SOLUTIONS

After Whitham (1955), let us introduce the following new variables to solve Equation (10) without linking the density  $\rho$  of inundation water to the friction factor  $K$  of inundation flow with sediment on a movable bed:

$$\alpha = \frac{K}{h_1} \left( 2c_1 t - \frac{1}{2}igt^2 - a \right) \quad (11) \quad \tau = \sqrt{\frac{g}{h_1}} Kt \quad (12)$$

where  $\alpha \geq 0$  and indicates a dimensionless distance between the tip position of inundation flow without and with sediment. By introducing these new variables, Equation (10) becomes

$$\left( \frac{d\alpha}{d\tau} \right)^3 \left( \frac{d^2\alpha}{d\tau^2} \right) \tau + \frac{1}{4} \frac{\rho_w}{\rho} \left( \frac{d\alpha}{d\tau} \right)^4 + 8 \left\{ \alpha - \frac{3}{2} \frac{d\alpha}{d\tau} \tau \right\} \left( 2 - \frac{i}{K} \tau - \frac{d\alpha}{d\tau} \right)^2 = 0 \quad (13)$$

Further, let us introduce the following variable conversions after Whitham (1955):

$$p = \frac{d\alpha}{d\tau} \quad (14) \quad \tau = f'(p) = \frac{df}{dp} \quad (15)$$

where  $p$  ( $0 \leq p \leq 2$ ) indicates a dimensionless flow velocity. These variable conversions lead to the following relations:

$$\frac{d^2\alpha}{d\tau^2} = \frac{1}{d^2f/dp^2} \quad (16) \quad \alpha = p \frac{df}{dp} - f \quad (17)$$

Therefore, Equation (13) becomes the following ordinary differential equation for  $f(p)$ :

$$p^3 f' + \frac{1}{4} \frac{\rho_w}{\rho} p^4 f'' - 8 \left\{ f + \frac{1}{2} p f' \right\} \left( 2 - \frac{i}{K} f' - p \right)^2 f'' = 0 \quad (18)$$

Let us assume that the dependent variable  $f(p)$  can be expanded into a power series of  $p$  as follows:

$$f(p) = \sum_{n=0}^{\infty} b_n p^n \quad (19)$$

From the initial condition that  $\alpha = da/dt = 0$  at  $\tau = 0$  ( $t = 0, p = 0$ ),  $b_0 = b_1 = 0$  is obtained. Substituting Equation (19) into Equation (18),  $b_2 = b_3 = 0$  and the following identical equation are obtained:

$$\begin{aligned} & (4b_4 + 5b_5 p + 6b_6 p^2 + 7b_7 p^3 + \dots) p^6 + \frac{\rho_w}{\rho} \left( 3b_4 + 5b_5 p + \frac{15}{2} b_6 p^2 + \frac{21}{2} b_7 p^3 + \dots \right) p^6 \\ & - \left[ 1,152b_4^2 + 192(17b_4 b_5 - 6b_4^2) p + 32(9b_4^2 - 102b_4 b_5 + 138b_4 b_6 + 70b_5^2) p^2 \right. \\ & \left. + 16 \left( 51b_4 b_5 - 276b_4 b_6 + 360b_4 b_7 - 140b_5^2 + 370b_5 b_6 - 288 \frac{i}{K} b_4^3 \right) p^3 + \dots \right] p^6 = 0 \end{aligned} \quad (20)$$

Solving this identical equation, Equations (21) to (25) are obtained as the coefficients  $b_4$  to  $b_8$ :

$$b_4 = \frac{1}{1,152} \left( 4 + 3 \frac{\rho_w}{\rho} \right) \quad (21) \quad b_5 = \frac{1,152b_4^2}{(3,264b_4 - 5 - 5\rho_w/\rho)} \quad (22) \quad b_6 = \frac{64(9b_4^2 - 102b_4 b_5 + 70b_5^2)}{(12 + 15\rho_w/\rho - 8,832b_4)} \quad (23)$$

$$b_7 = \frac{32(51b_4 b_5 - 276b_4 b_6 - 140b_5^2 + 370b_5 b_6 - 288b_4^3 i/K)}{(14 + 21\rho_w/\rho - 11,520b_4)} \quad (24)$$

$$b_8 = \frac{8(69b_4 b_6 - 360b_4 b_7 + 35b_5^2 - 370b_5 b_6 + 474b_5 b_7 + 240b_6^2 + 24b_4^2(6b_4 - 49b_5)i/K)}{(4 + 7\rho_w/\rho - 3,648b_4)} \quad (25)$$

From the above results, the following series solutions to the tip position  $a(t)$ , velocity  $U(t)$  and acceleration  $d^2a/dt^2$  of inundation flow with sediment on a movable bed are obtained for any  $h_1, i, K$ :

$$a = 2c_1 t - \frac{1}{2} i g t^2 - \frac{h_1}{K} (3b_4 p^4 + 4b_5 p^5 + 5b_6 p^6 + 6b_7 p^7 + \dots) \quad (26)$$

$$U = \frac{da}{dt} = 2c_1 - i g t - c_1 p \quad (27)$$

$$\frac{d^2a}{dt^2} = -i g - \frac{K g}{12b_4 p^2 + 20b_5 p^3 + 30b_6 p^4 + 42b_7 p^5 + \dots} \quad (28)$$

$$t = \frac{1}{K} \sqrt{\frac{h_1}{g}} (4b_4 p^3 + 5b_5 p^4 + 6b_6 p^5 + 7b_7 p^6 + \dots) \quad (29)$$

### Examples of Series Solutions and Discussions

Figure 2 shows an example of convergence of Equations (26) and (29) which are the series solution to the tip position  $a(t)$  of inundation flow with sediment, where the friction factor  $K$  is not linked to the density  $\rho$  of inundation water. From the figure, it can be seen that adopting the 5<sup>th</sup> order approximate solution to the coefficient  $b_8$ , the series solution to  $a(t)$  converges with enough accuracy, e.g., the difference between the 4<sup>th</sup> and 5<sup>th</sup> order approximate solutions to the maximum run-up distance  $a_m$  is around 4.6%. Therefore, the 5<sup>th</sup> order approximate solutions are adopted below. Figure 2 also indicates that the trajectory of the tip position  $a(t)$  in the run-up and backwash processes is not axisymmetric.

Figures 3 and 4 show the dependencies of the tip position  $a(t)$  evaluated from the 5<sup>th</sup> order approximate solution on the friction factor  $K$  and the density  $\rho$  (or  $\rho/\rho_w$ ), respectively. From the figures, it can be seen that (1) not only the maximum run-up distance  $a_m$  but also the time required for the maximum run-up distance and the duration time of  $a(t) > 0$  depend on the friction factor  $K$ , (2) when only the density  $\rho$  changes independently of the friction factor  $K$ , influence of the density  $\rho$  on the maximum run-up distance  $a_m$  is small, compared with the experimental results (Matsutomi and Konno

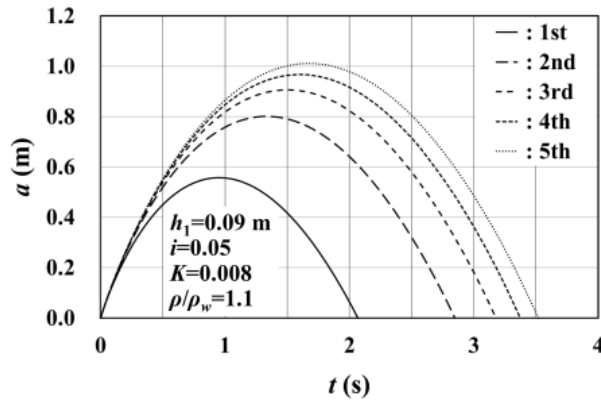


Figure 2. A convergence example of the series solution to the tip position  $a(t)$  of inundation flow.

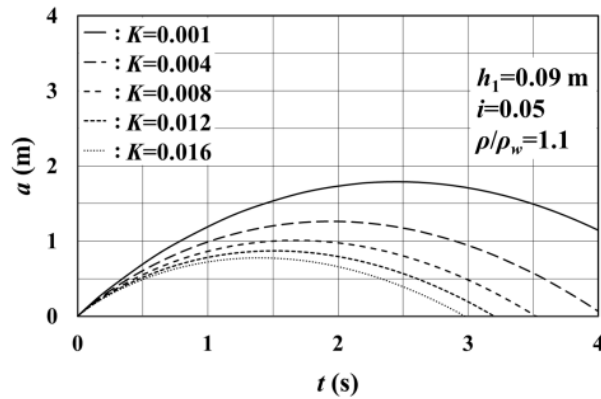


Figure 3. Dependency of the tip position  $a(t)$  on the friction factor  $K$  of inundation flow (5<sup>th</sup> order approximation).

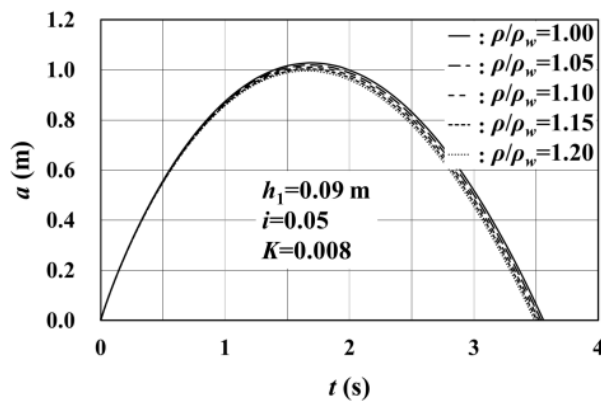


Figure 4. Dependency of the tip position  $a(t)$  on the density  $\rho$  of inundation water (5<sup>th</sup> order approximation).

2019) (see Figure 8 discussed later). The latter (2) strongly suggests that linking the friction factor  $K$  to the density  $\rho$  is important in the estimation of the tip position  $a(t)$  of inundation flow with sediment over a movable bed.

Figures 5 to 7 show examples of time histories of the tip position  $a(t)$  and rear position  $\zeta(t)$  of the tip region, inundation water depth  $H(t)$  at  $\zeta(t)$ , inundation flow velocity  $U(t)$  and acceleration  $d^2a/dt^2$  in the tip region and incident Froude number  $F_{ri}$  (which is always positive, but is displayed considering the direction of  $U(t)$ ) at  $\zeta(t)$ , evaluated from the 5<sup>th</sup> order approximate solutions. Although the time histories of  $F_{ri}$  and  $d^2a/dt^2$  at early stage are omitted in Figure 7, they asymptotically approach  $\pm\infty$  respectively.

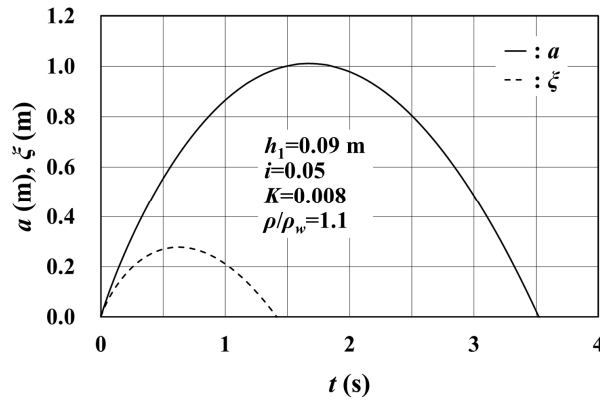


Figure 5. Time histories of the tip position  $a(t)$  and rear position  $\zeta(t)$  of the tip region (5<sup>th</sup> order approximation).

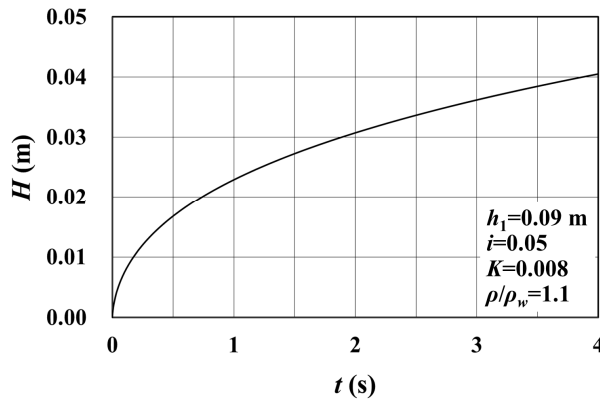


Figure 6. Time history of the inundation water depth  $H(t)$  at the rear position  $\zeta(t)$  (5<sup>th</sup> order approximation).

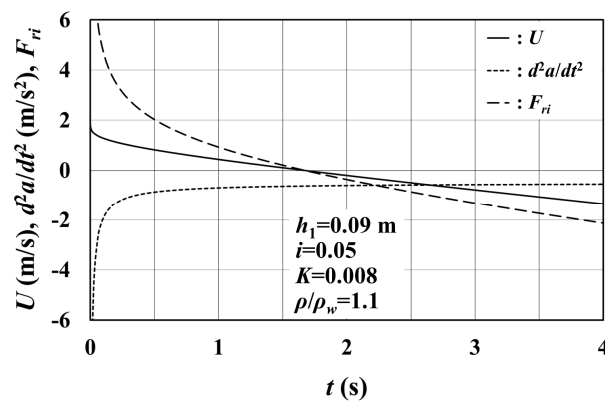


Figure 7. Time histories of the inundation flow velocity  $U$  ( $=da/dt$ ) and acceleration  $d^2a/dt^2$  in the tip region, and incident Froude number  $F_{ri}$  at the rear position  $\zeta(t)$  (5<sup>th</sup> order approximation).

From the figures, it can be seen that rapidly, (1) the tip region ( $=a(t)-\zeta(t)$ ) expands, (2) inundation water depth  $H(t)$  at  $\zeta(t)$  increases in a upward convex curved shape, (3) acceleration  $d^2a/dt^2$  and incident Froude number  $F_{ri}$  decrease and gradually approach to  $-ig$  and  $-\infty$  respectively in the series solutions.

**ANALYTICAL SOLUTIONS**

In the preceding chapter, it was pointed out that linking the friction factor  $K$  to the density  $\rho$  of inundation water was important in the run-up analysis of inundation flow with sediment on a movable bed.

According to Matsutomi (2019), the density  $\rho$  of inundation water can be estimated by both the friction factor  $K$  of inundation flow with sediment on a movable bed and incident Froude number  $F_{ri}$  of inundation flow as shown in Equation (30):

$$\rho = \frac{\rho_w}{1 - KF_{ri}^2} \quad (30)$$

Therefore, discussion of the density  $\rho$  of inundation flow with sediment on a movable bed is nothing but that of the friction factor  $K$  of inundation flow.

In this study, incident Froude number  $F_{ri}$  is defined by adopting inundation flow velocity  $U(t)$  in the tip region and long wave celerity  $C$  at the rear position  $\zeta(t)$  of the tip region as shown in Equations (31) and (32).

$$F_{ri} = \frac{U}{C} \quad (31) \quad C = \sqrt{gH} = \frac{1}{3} \left( 2c_1 - \frac{\zeta}{t} - \frac{1}{2}igt \right) \quad (32)$$

Equation (33) is derived from Equations (31), (32) and (9):

$$F_{ri} = \frac{2U}{2c_1 - U - igt} \quad (33)$$

Therefore, the friction factor  $K$  can be expressed as follows:

$$K = \left( 1 - \frac{\rho_w}{\rho} \right) \frac{1}{F_{ri}^2} = \left( 1 - \frac{\rho_w}{\rho} \right) \frac{(2c_1 - U - igt)^2}{4U^2} \quad (34)$$

Substituting Equation (34) into Equation (10), Equation (35) is obtained as the basic equation, without having the friction factor  $K$ , to be solved in this chapter:

$$\begin{aligned} & \left( c_1 - \frac{1}{2} \frac{da}{dt} - \frac{1}{2}igt \right) t \frac{d^2a}{dt^2} - \frac{1}{2} \frac{\rho_w}{\rho} \left( c_1 - \frac{1}{2} \frac{da}{dt} - \frac{1}{2}igt \right)^2 \\ & + ig \left( c_1 - \frac{1}{2} \frac{da}{dt} - \frac{1}{2}igt \right) t + \left( 1 - \frac{\rho_w}{\rho} \right) g \left\{ a - \left( \frac{3}{2} \frac{da}{dt} - c_1 + igt \right) t \right\} = 0 \end{aligned} \quad (35)$$

After the preceding chapter, let us introduce the following new variables without having the friction factor  $K$  of inundation flow with sediment on a movable bed to solve Equation (35):

$$\alpha = \frac{1}{h_1} \left( 2c_1 t - \frac{1}{2}igt^2 - a \right) \quad (36) \quad \tau = \sqrt{\frac{g}{h_1}} t \quad (37)$$

Using these new variables, Equation (35) becomes

$$\frac{d\alpha}{d\tau} \frac{d^2\alpha}{d\tau^2} \tau + \frac{1}{4} \frac{\rho_w}{\rho} \left( \frac{d\alpha}{d\tau} \right)^2 + 2 \left( 1 - \frac{\rho_w}{\rho} \right) \left( \alpha - \frac{3}{2} \frac{d\alpha}{d\tau} \tau \right) = 0 \quad (38)$$

Introducing the variable conversions of Equations (14) and (15) as the preceding chapter, Equation (38) becomes

$$pf' + \frac{1}{4} \frac{\rho_w}{\rho} p^2 f'' - 2 \left( 1 - \frac{\rho_w}{\rho} \right) \left( f + \frac{1}{2} pf' \right) f'' = 0 \quad (39)$$

Equation (39) is solved assuming a series solution of  $p$  as Equation (19).

From the initial condition that  $\alpha = da/dt = 0$  at  $\tau = 0$  ( $t = 0, p = 0$ ),  $b_0 = b_1 = 0$  is obtained. Substituting Equation (19) into Equation (39), the following identical equation is obtained:

$$\begin{aligned} & (2b_2 + 3b_3p + 4b_4p^2 + 5b_5p^3 + 6b_6p^4 + \dots)p^2 \\ & + \frac{1}{4} \frac{\rho_w}{\rho} (2b_2 + 6b_3p + 12b_4p^2 + 20b_5p^3 + 30b_6p^4 + \dots)p^2 \\ & - 2 \left( 1 - \frac{\rho_w}{\rho} \right) \left( 4b_2^2 + 17b_2b_3p + (30b_2b_4 + 15b_3^2)p^2 + (47b_2b_5 + 48b_3b_4)p^3 \right. \\ & \left. + (68b_2b_6 + 71b_3b_5 + 36b_4^2)p^4 + \dots \right) p^2 = 0 \end{aligned} \quad (40)$$

Solving the above identical equation, Equations (41) and (42) are obtained as the coefficients of series solution:

$$b_2 = \frac{1}{16} \frac{(4 + \rho_w/\rho)}{(1 - \rho_w/\rho)} \quad (41) \quad b_3 = b_4 = b_5 = b_6 = \dots = 0 \quad (42)$$

These results indicate that analytical solution can be derived without assuming the series solution to  $f(p)$ . Therefore, the tip position  $a(t)$  of inundation flow with sediment is expressed as follows:

$$a = 2c_1 t - \frac{1}{2}igt^2 - h_1(b_2 p^2) \quad (43) \quad t = \sqrt{h_1/g} (2b_2 p) \quad (44)$$

From the above results, the following analytical solutions to the tip position  $a(t)$ , velocity  $U(t)$  and acceleration  $d^2a/dt^2$  of inundation flow with sediment on a movable bed are obtained for any  $h_1$  and  $i$ :

$$a = 2c_1t - \frac{1}{2}igt^2 - 4\frac{(1-\rho_w/\rho)}{(4+\rho_w/\rho)}gt^2 \quad (45)$$

$$U = \frac{da}{dt} = 2c_1 - igt - 8\frac{(1-\rho_w/\rho)}{(4+\rho_w/\rho)}gt \quad (46)$$

$$\frac{d^2a}{dt^2} = -ig - 8\frac{(1-\rho_w/\rho)}{(4+\rho_w/\rho)}g \quad (47)$$

When the density  $\rho$  is a constant, trajectories of the tip position  $a(t)$  and inundation flow velocity  $U(t)$  are a parabola and a linear decreasing monotonically, respectively.

From Equations (6), (9) and (46), the following is obtained as the inundation water depth  $H(t)$  at the rear position  $\zeta(t)$  of the tip region, which is a parabola and discussed later:

$$H = 16\left(\frac{1-\rho_w/\rho}{4+\rho_w/\rho}\right)^2gt^2 \quad (48)$$

The following analytical solutions to the maximum run-up distance  $a_m$  and height  $R_m$  of inundation flow with sediment on a movable bed are also obtained for any  $h_1$  and  $i$ :

$$\frac{ia_m}{h_1} = \frac{R_m}{h_1} = \frac{2}{1+(8/i)(1-\rho_w/\rho)/(4+\rho_w/\rho)} \quad (49)$$

### Examples of Analytical Solutions and Discussions

Figure 8 shows the dependency of the tip position  $a(t)$  evaluated from the analytical solution (Equation (45)) on the density  $\rho$  (or  $\rho/\rho_w$ ) of inundation water. In reality, the density  $\rho$  as well as the friction factor  $K$  of inundation flow depends on the time  $t$ . In the figure, the solid line is nothing but Equation (8) for the tip position  $x_s$  of frictionless inundation flow which cannot take in sediment from a movable bed. The figure tells that as the density  $\rho$  becomes high, not only the maximum run-up distance  $a_m$  of inundation flow but also the time required for the maximum run-up distance  $a_m$  and the duration time of  $a(t)>0$  become short. These tendencies are the same as those in case of that the friction factor  $K$  increases as shown in Figure 3. It can be also seen through a comparison with the results shown in Figure 3, which are obtained by adopting the friction factor  $K$  having a constant value averaged over the whole process of run-up and backwash of inundation flow, that the results shown in Figure 8 indicate the run-up duration time becomes short for the maximum run-up distance  $a_m$ . This suggests that it is necessary to adopt friction factor  $K$  changing every moment in accordance with the situation of inundation flow with sediment.

Figure 9 shows the dependency of the dimensionless run-up height  $R_m/h_1$  evaluated from the analytical solution (Equation (49)) on the density  $\rho$  (or  $\rho/\rho_w$ ) of inundation water, using the bottom slope  $i$  as a parameter. The figure tells that the dimensionless run-up height  $R_m/h_1$  strongly depends on both the density  $\rho$  and the bottom slope  $i$ .

Figures 10 to 12 show examples of time histories of the tip position  $a(t)$  and rear position  $\zeta(t)$  of the tip region, inundation water depth  $H(t)$  at  $\zeta(t)$ , inundation flow velocity  $U(t)$  and acceleration  $d^2a/dt^2$  in the tip region and incident Froude number  $F_{ri}$  at  $\zeta(t)$ , evaluated from the analytical solutions. In these time histories, there is an attention point that the time history of the inundation water depth  $H(t)$  at  $\zeta(t)$  is a downward convex curved shape (a upward convex curved shape in the series solution) and the inundation water depth  $H(t)$  becomes a physically impossible large value after a midway of backwash process of inundation flow. One of the reasons for such a tendency of the inundation water depth  $H(t)$  lies in the introduction of Equation (30). When average density over the run-up process of inundation flow is adopted as the density  $\rho$  in Equation (30), the friction factor  $K$  ( $<1/F_{ri}^2$ ) in Equation (30) becomes small (large) with increase (decrease) of incident Froude number  $F_{ri}$ . Therefore, compared with the case of the series solutions in which the friction factor  $K$  is a constant value, the inundation flow velocity  $U(t)$  in the tip region is large in early stage of run-up process and is quickly decreased near the maximum run-up distance  $a_m$  (see Figures 7 and 12), and as the result, the time history of inundation water depth  $H(t)$  becomes a downward convex curved shape. As seen from the fact that trajectory of the tip position  $a(t)$  is a parabola (see Equation (45)), the above situation of inundation flow velocity  $U(t)$  is the same even in the backwash process. For this reason, when inundation flow velocity  $U(t)$  decreases from 0 in the backwash process, inundation water depth  $H(t)$  increases as expressed in Equation (48) in response to the decreasing inundation flow velocity  $U(t)$ .

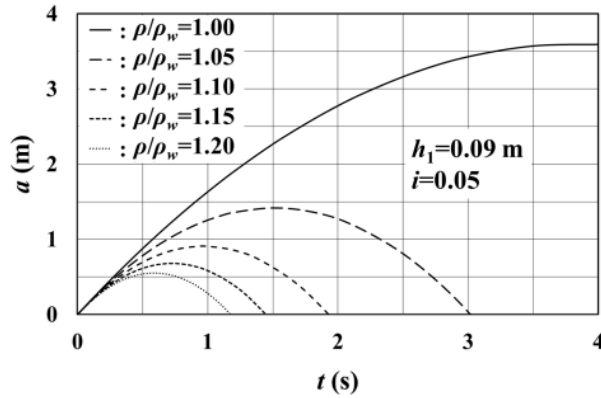


Figure 8. Dependency of the tip position  $a(t)$  of inundation flow on the density  $\rho$  (or  $\rho/\rho_w$ ) of inundation water (analytical solution).

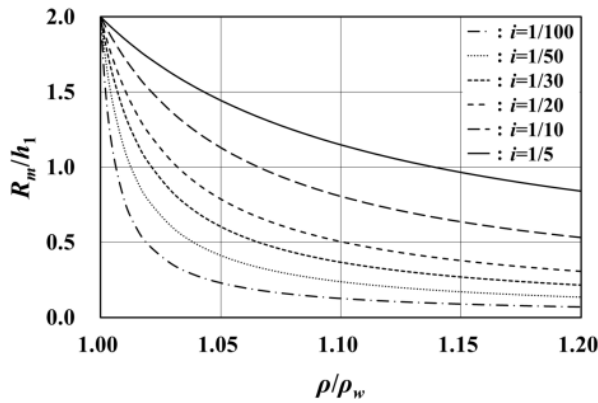


Figure 9. Dependency of the dimensionless run-up height  $R_m/h_1$  on the density  $\rho$  (or  $\rho/\rho_w$ ) and bottom slope  $i$  (analytical solution).

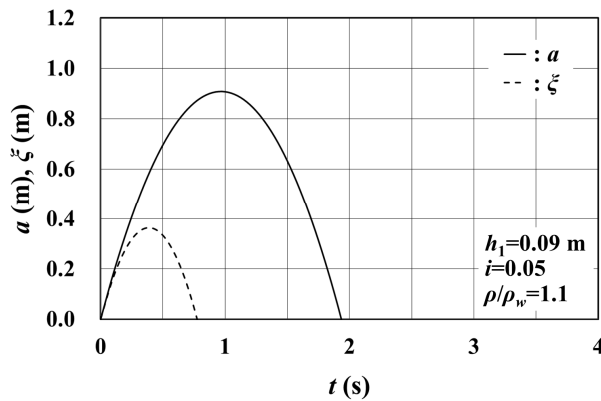


Figure 10. Time histories of the tip position  $a(t)$  and rear position  $\xi(t)$  of the tip region (analytical solution).

From the above, although the application range of the analytical solutions is restricted to a midway of backwash process of inundation flow, the application limit just hinder a part of the aims of this study. However, further improvements of both this approximate model of the tip region and operation of Equation (30) are expected.

#### VERIFICATION OF SOLUTIONS

A verification of validity of the series and analytical solutions is carried out through a comparison

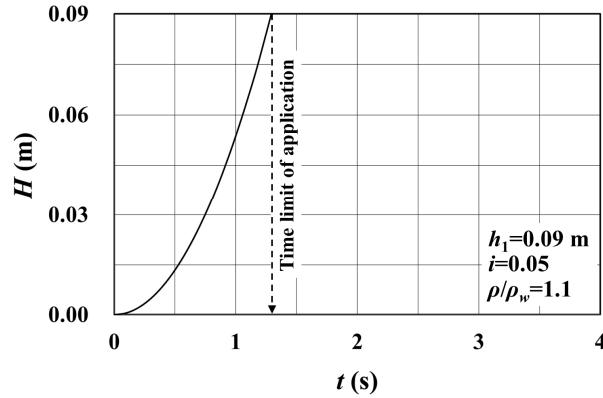


Figure 11. Time history of the inundation water depth  $H(t)$  at the rear position  $\xi(t)$  (analytical solution).

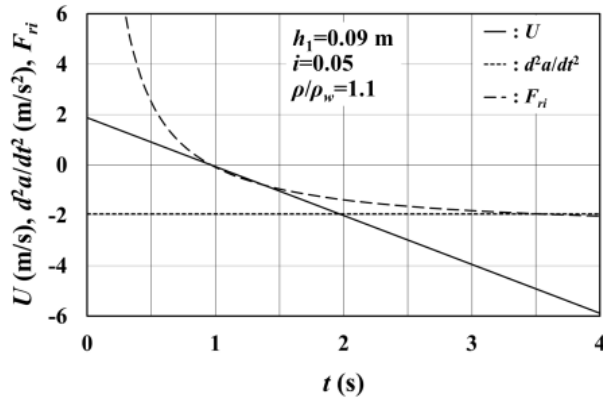


Figure 12. Time histories of the inundation flow velocity  $U (=da/dt)$  and acceleration  $d^2a/dt^2$  in the tip region, and incident Froude number  $F_{ri}$  at the rear position  $\xi(t)$  (analytical solution).

with experimental data. However, the verification is not strict because of lacks of experimental data under the same condition as the solutions.

Matsutomi and Konno (2019) presented some experimental data on the maximum run-up distance  $a_m$  of inundation flow with or without sediment. Table 1 and Figure 13 show a part of the experimental conditions and data, and outline of flume used in the experiments, respectively. In the table, the experimental case number is the same as that used in the reference (Matsutomi and Konno 2019),  $h_D$  the bottom height of water storage tank from the ground level,  $L_U$  the length of water storage tank,  $h_U$  the initial stored water depth in the water storage tank,  $h_T$  the initial thickness of soil layer spread in the horizontal flume,  $L_S$  the initial length of the spread soil region,  $h_S$  the height of the first short mild upward slope end from the ground level,  $i (=S_3$  in Figure 13) the bottom slope of the second long mild upward slope where inundation flow with or without sediment runs up.

Concrete verification procedure consists of the following three steps:

- Step 1: Estimate the stored water depth  $h_1$  from Equation (49) by adopting the values of  $\rho/\rho_w=1.122$  (average value of four times), bottom slope  $i=0.127$ , maximum run-up distance  $a_m=R_m/i=L_R=1.06$  m (average value of four times), where the definition of the experimental maximum run-up distance  $L_R$  is presented in Figure 13.
- Step 2: Estimate friction factor  $K$  in the case that inundation flow without sediment on a fixed bed under the condition of  $h_1$  estimated in Step 1 runs up the slope, on which sand with grain size 0.85 mm to 2 mm is pasted, used in the experiment (Matsutomi and Konno 2019).
- Step 3: Examine whether the maximum run-up distance  $L_{RW}$  is longer than  $L_R=1.06$  m or not, where  $L_{RW}$  is estimated by substituting  $\rho/\rho_w=1.0$ ,  $i=0.127$ ,  $h_1$  estimated in Step 1 and  $K$  estimated in Step 2 into the series solution (Equations (26) and (29)) of 5th order approximation to the maximum run-up distance  $a_m$  of inundation flow without sediment. This examination can also be regarded as an integrity verification of the analytical and series solutions.



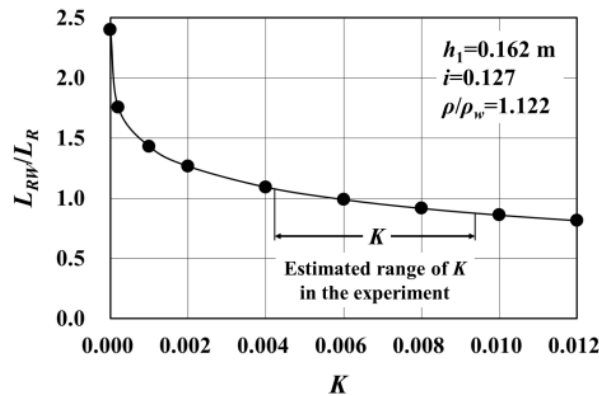


Figure 14. Ratio  $L_{RW}/L_R$  of the maximum run-up distance  $L_{RW}$  of inundation flow without sediment evaluated every  $K$  ( $\rho/\rho_w=1.0$ , 5<sup>th</sup> order approximation) to the maximum run-up distance  $L_R$  obtained by experiment.

As reasons for that the series solution to the maximum run-up distance  $a_m$  gives shorter than expected, it would be considered that (1) friction factor  $K$  is kept constant in the run-up process, (2) accuracy of the estimated value of  $K$  and the experimental values adopted are low. Now, I strongly realize the necessity of experimental data more suitable for comparison with the solutions derived in this study.

## CONCLUSIONS

Main results obtained by this study are that:

1. Series solutions to the tip position  $a(t)$  (Equations (26) and (29)), velocity  $U (=da/dt)$  and acceleration  $d^2a/dt^2$  in the tip region of inundation flow with sediment on a movable bed uniformly sloped under the condition that the friction factor  $K$  was not linked to the density  $\rho$  of inundation water, and analytical solutions to  $a(t)$  (Equation (45)),  $U(t)$  (Equation (46)),  $d^2a/dt^2$  (Equation (47)), the maximum run-up distance  $a_m$  and height  $R_m$  (Equation (49)) under the condition that  $K$  was linked to  $\rho$  were derived, and effects of  $\rho$  on them and run-up process were examined (Figures 3 to 12).
2. It was indicated that in the run-up analysis (including numerical simulation) of tsunami with sediment on a movable bed under the condition of a constant  $K$ , even if the maximum run-up distance  $a_m$  and run-up height  $R_m$  could be predicted accurately, there was a possibility of evaluating the run-up duration time inaccurately and vice versa (Figures 3 and 8), and linking  $K$  to  $\rho$  was necessary to solve this matter. An expression for the relationship between  $K$  and  $\rho$  was also presented (Equation (30)).
3. It was verified that the derived series and analytical solutions were useful to discuss the effects of  $\rho$  on the run-up of tsunami with sediment on a movable bed through a comparison between the experimental and theoretical maximum run-up distances.

## ACKNOWLEDGMENTS

This work was supported by JSPS the Grant-in-Aid for Scientific Research (C) Grant Numbers JP20K05041.

## REFERENCES

- Kelly, D. M., and N. Dodd. 2010. Beach-face evolution in the swash zone, *JFM*, 661, 316-340.
- Matsutomi, H. 1985. On the propagation of a bore over a sloping beach, *Coastal Engineering in Japan*, 28, 45-58.
- Matsutomi, H. 2003. Dam-break Flow over a Uniformly Sloping Bottom, *J. Hydraul., Coast. Environ. Eng.*, JSCE, 726/II-62, 151-156.
- Matsutomi, H., and S. Kawashima. 2015. Elementary experiment on the maximum density of tsunami inundation flow, *Journal of JSCE*, B2, 71, 2, 355-360. (in Japanese)
- Matsutomi, H. 2019. A simple method for evaluating the density of tsunami inundation water, *Journal of JSCE*, B2, 75, 2, 385-390. (in Japanese)

- Matsutomi, H., A. Mikami, and Y. Chiba. 2019. Influence of the tsunami inundation water density and wave period on the tsunami load on RC building, *Journal of JSCE*, B2, 75, 2, 397-402. (in Japanese)
- Matsutomi, H., and F. Konno. 2019. Experiments on the density of tsunami inundation water and its influence on the tsunami run-up and deposit, *Proc. of ICCE*, 36, Full Length Paper.41.
- Peregrine, D. H., and S. M. Williams. 2001. Swash overtopping a truncated plane beach, *JFM*, 440, 391-399.
- Shen, M. C., and R. E. Meyer. 1963. Climb of a bore on a beach, Part 3: Run-up, *JFM*, 16, 113-125.
- Whitham, G. B. 1955. The effects of hydraulic resistance in the dam-break problem, *Proc. Roy. Soc.*, 227, 399-407.